Energy Recovery from Domestic Radiators using a Compact Composite Metal Foam/PCM Latent Heat Storage

Pouyan Talebizadeh Sardari[1,*], Rohollah Babaei-Mahani[2], Donald Giddings[1], Sirous Yasseri[3], Moahammad Moghimi Ardekani[4], Hamid Bahai[3]

[1]Faculty of Engineering, University of Nottingham, University Park, Nottingham NG7 2RD, United Kingdom.

[2]Director, Belmore Energy Ltd., London, United Kingdom.

[3]Department of Mechanical and Aerospace Engineering, Brunel University London, Howell Building, Brunel University, Uxbridge, UB8 3PH, United Kingdom.

[4]Department of Design and Engineering, Staffordshire University, Stoke-on-Trent, ST4 2DE, United Kingdom.

Abstract

With increasing demand for energy consumption in domestic buildings and consequent CO_2 emission, there is a need to provide proper products to reduce energy loss. Domestic radiators for space heating can be improved by using Compact Latent Heat Storage (CLHS) mounted on the wall side surface in order to offer energy saving and peak-shaving. The unit offer potential to save otherwise wasted energy from the back surface of the radiator to the walls in the charging mode. When the heating system is turned off, the CLHS unit discharge the stored heat towards the room. An aluminium foam embedded inside the bulk Phase Change Material (PCM) can enhance the heat storage/retrieval rate. A PCM is selected depending on the radiator's surface temperature, which is almost equal to the hot water temperature delivered to the radiator. Different metal foam porosity is examined and compared with the PCM-only alternative (i.e. without foam enhancement). The results show the porous-PCM CLHS alternative provides an almost constant temperature during the discharging process equal to

* Corresponding author.

E-mail address: pouyan.talebizadehsardari@nottingham.ac.uk (P. Talebizadeh Sardari).

54℃. However, for the PCM-only alternative, the temperature of the surface reduces continuously. Using the porous medium results in a shorter melting time, about 95% of what is needed for the PCM-only alternative. Increasing the metal foam porosity results in shorter charging/discharging time; however, since the surface temperature of the porous-PCM unit is almost constant for different porosity of the metal foam, a system with higher porosity (97%) is desirable.

Keywords: Latent heat storage; Compact design; Phase change material; Porous medium, Radiator; Charging/discharging.

Nomenclature

A_m	Mushy zone	Ra	Rayleigh number
C	Inertial coefficient	t_m	Charging/Discharging time (s)
C_p	PCM Specific heat (J/kg.K)	T	Temperature (K)
e_e	Total energy at the end of charging/discharging process (J)	T_e	Temperature at the end of charging/discharging process(K)
e_i	Total energy at the initial of charging/discharging process (J)	T_i	Initial temperature (K)
g	Gravity (m/s^2)	T_{ref}	Reference temperature (K)
H	Height of the unit (m)	$\vec{V}$	Velocity vector (m/s)
k_{pcm}	Fluid Thermal conductivity (PCM) (W/m.K)		
k_{porous}	Porous medium Thermal conductivity (W/m.K)	**Greek symbols**	
K	Permeability (m^2)	β	Thermal expansion coefficient of PCM (1/K)
L	Fusion Latent heat of PCM (J/kg)	ε	Porosity
m	PCM mass (kg)	λ	Liquid fraction
P	Pressure (Pa)	μ	Dynamic viscosity of PCM (kg/m.s)
Pr	Prandtl number	ρ	PCM Density (kg/m^3)
Q	Capacity of heat storage/retrieval (J)	ΔH	Latent heat (J/kg)
$\dot{Q}$	Rate of heat storage/retrieval (W)	ΔP	Pressure drop (Pa)

1. Introduction

New technologies recovering heat from domestic space and water heating could make a significant impact on the energy consumption and CO_2 reduction while improving the quality of life (Yu et al., 2019). Among all energy consumed by end users, domestic space heating accounts for 45-47% and water heating accounts for another 40% (Marique et al., 2014). In the UK, buildings were responsible for 29% of the total final energy consumption in 2015 according to the department for Business, Energy and Industrial Strategy which increased by 3.1% in 2016 (BIES, July 2017). In 2016, the residential sector is accounted for 18% of all CO_2 emissions which is 4.5% higher than 2015 (BEIS, March 2017). Any attempt to reduce the consumption, without impacting the quality of life, or even curb it will be beneficial to the nation and also benefits the environment (Irshad et al., 2019). Recovery and storing heat can contribute substantially toward this goal (Yong et al., 2016).

Among different storage technologies, Thermal Energy Storage (TES) provides an effective peak shaving technology used in thermal energy demand, efficient use of energy, recovery from low-grade heat waste, as well as uniformity of the distributed energy and backup energy systems. In Europe, around 1.4 million GWh/year and 400 million tons of CO_2 emissions are estimated to be saved by TES (Sarbu and Sebarchievici, 2016). Considering different TES types, Latent heat storage (LHS) systems have great potential to provide a cost-effective solution for this problem. Phase change materials (PCMs) are used in LHS systems to store heat during the melting process and then release heat during the solidification process. PCMs are also capable to compete with other sensible heat storage materials such as MgO in terms of cost per kWh, and are far more compact and also cheaper than electrochemical thermal storages. They have an energy density typically 5 to 14 times higher than any rival heat storage systems and have the added advantage of almost constant temperature during the phase changing process (Khan et al., 2016). Thus, this is a significant national importance to the UK energy needs, economy, and quality of life.

The main challenges for efficient use of PCM-based technology are the long melting/solidification time as well as inefficient releasing/gaining heat due to low thermal conductivity and low thermal diffusivity within the bulk PCM (Sheikholeslami, 2018a); these disadvantages led to limited use of LHS systems in the past (Pereira da Cunha and Eames, 2016). However, among different enhancement methods for the heat storage/retrieval rate including geometry modification (Dadollahi and Mehrpooya, 2017), use of fins (Wang and Yang, 2011), use of nanoparticles (Sheikholeslami, 2018b), use of encapsulation (Jamekhorshid et al., 2014) and use of porous structures (Zhao, 2012), employing high conductive metal foam is proving to be a promising technology to solve this problem.

In the composite porous/PCM combination, the heat is transferred by conduction through the high conductivity of the porous foam rather than PCM which increases the rate of thermal diffusion (Shahsavar et al., 2019). It was shown that the effect of conduction heat transfer by the porous foam is to significantly enhance the performance of the charging/discharging process (Zhang et al., 2017). Py et al. (2001) presented that the effective thermal-conductivity of paraffin-based heat storage with graphite foam increased to the range from 4 to 70 W/mK instead of 0.24 W/mK as the thermal-conductivity of paraffin only. Zhao et al. (2010) studied the effects of the Cu metal foam on the phase change rate of RT58 and they stated that the metal foam can enhance the phase-change rate around 10 times depending on the material and the conditions. Mesalhy et al. (2005) recommended a PCM storage with high porosity and high thermal conductivity due to the reduction of the convection effect due to the use of the porous medium. Liu et al. (2013) studied numerically the melting of a composite metal foam/PCM shell and tube storage for 2-D and 3-D cases. They showed the low effect of pore size on the melting process and negligible effect of natural convection because of high flow resistance in the porous medium. Nithyanandam et al. (2014) numerically studied the effect of the metal foam on the LHS system based on heat pipes. They found that lower pore size improves the

rate of heat transfer. Mahdi et al. (2018) studied a 2D double tube LHSHX using multiple-segment metal foam with various porosity. They presented that the use of different foam porosity in different segments enhances the rate of heat storage and recovery compared with the single porosity case. Shahsavar et al. (2019) employed the geometry modification simultaneous with the porous medium to enhance the heat transfer of cylindrical LHS unit showing more than 90% reduction in melting/solidification times. Sheikholeslami and Mahian (Sheikholeslami and Mahian, 2019) studied the effect of magnetic field on the solidification process of a nano-PCM embedded in a porous annulus. They showed that the addition of nanoparticles reduce the solidification time by 14% while applying the magnetic field enhances the solidification process by 23.5%.

There are a few studies reported on the application of latent heat storage heat exchangers (LHSHE) for room heating and ventilation in the literature (Campos-Celador et al., 2014). Wang et al. (2006) performed an experimental study on a type of high-temperature latent heat storage air heater in a room with the aim of providing electricity for peak hours from off-peak hours. They used electrical elements to charge the PCM with high latent heat and high melting point. The results show that by charging the system for 8 hours, the system can provide suitable heat for room heating in the remaining 16 hours. Dechesne et al. (2014) studied a PCM air heat exchanger in a ventilation system. In their study, the heat gained from the Photovoltaic modules is stored during the day and released to the room during the night. For cooling purpose, coolness is stored during the night and released to the room during the day. They developed a semi-empirical equation for the outlet temperature of the air. The system can provide more than 50 W of cooling and heating powered by the PCM heat exchanger over five hours. Osterman et al. (2015) prepared PCM storage unit suitable for both cooling and heating purposes. During summer, the system stores cold from the outdoor air at night to reduce the required cooling load during the daytime. During winter, the system stores heat from the air heated by solar

collectors. They showed, annually 142 kWh energy consumption of an office can be saved. Wang et al. (2015) studied a PCM air heat exchanger with a zigzag plate geometry using different unequal mass PCMs with various melting points. They validated their model with the experimental data using NaCl-$MgCl_2$ salt. They showed the advantage of using a combination of PCMs instead of PCM-only. They showed that there is a time period within which the outlet temperature is almost equal to the initial temperature depending on the melting points of the employed PCM. It is noteworthy that although there have been some studies on the use of PCM for space heating in the literature, the use of composite metal foam/PCM for room heating purposes has not received attention; which can solve the problem of low thermal diffusivity of pure PCMs.

The aim of this paper is to employ a composite metal foam-PCM in compact latent heat storage (CLHS) unit adapted for commercially available radiators. The potential of a CLHS unit to save more energy recovered from typical radiators is presented for domestic space heating. For this purpose, the system is designed to be fitted in the space at the back of the radiator. Aluminium foam is employed to enhance the rate of heat transfer inside the PCM. The objective is to find if the system can provide a uniform temperature on the radiator's surface during the discharging process. Furthermore, the system is analysed in the charging process to determine the charging time. The idea that is introduced for the first time in this paper can be added to existing heating systems and can contribute significantly to energy saving and peak shaving opportunities in buildings with the consequent reduction of associated energy production emissions.

2. System description

The objective of this study is to develop a model of a compact composite storage unit that can be added to the back of current radiators. The CLHS unit's dimensions were obtained based on the size of a commercially available radiator and the possible space at the back of the radiator. It is a rectangular thin enclosure, which is thin enough to be placed at the back of a radiator to store excess heat, and release heat when the boiler is turned off; aiming to maintain the constant temperature on the radiator surface. The schematic of the entire system is displayed in Fig. 1. It is worth mentioning that for fabrication of the composite metal foam-PCM unit, in a vacuumed environment, the PCM is melted and penetrated inside the pores of the foam and then is solidified to make the composite block. Detailed description of the method exist in the literature (Shang et al., 2018; Xiao et al., 2013)

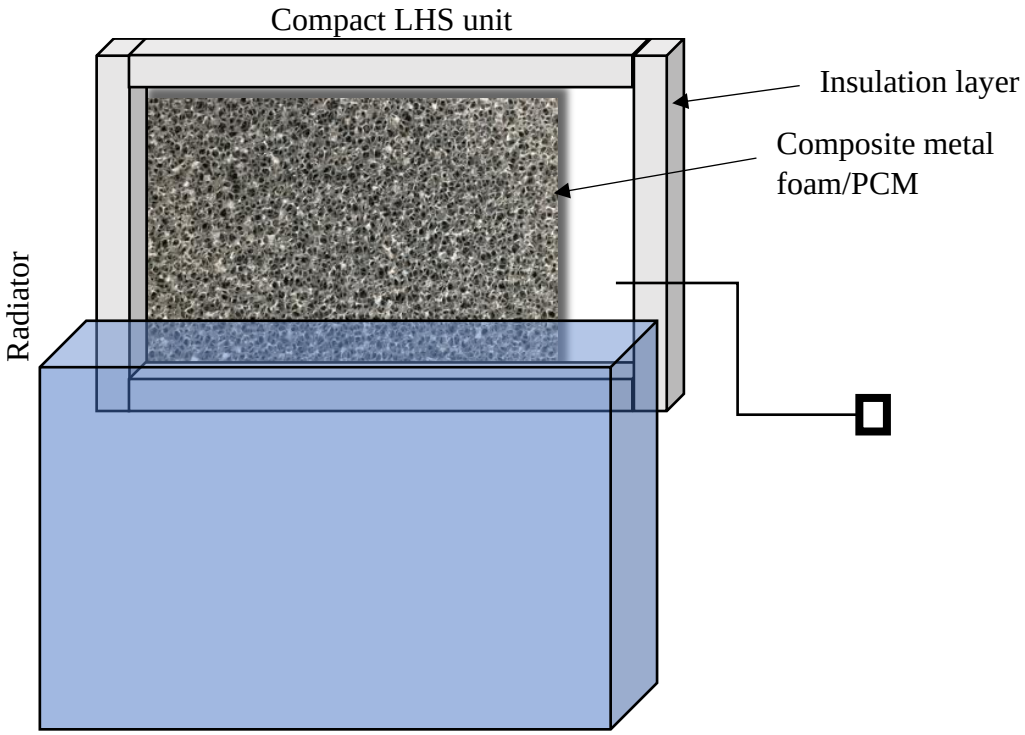

Fig. 1. The schematic of the studied system

The dimensions of the LHS unit are 100cm×50cm×2cm. This is a thin unit so that it can be installed in the space at the back of radiators. The LHS unit includes an Aluminium foam with the pore density of 30PPI and RT54HC as the PCM. The porous-PCM alternative with different porosities is compared with the PCM-only alternative. Note all the surfaces of the LHS, except the front wall, are considered as adiabatic. Constant temperature and convection heat transfer are considered as the front wall boundary condition in the charging and discharging mechanisms, respectively. The detailed description of the boundary conditions is presented in Section 4. In addition to the novel proposed application, this study assesses the effect of the porous medium in a low thickness heat storage system. It should be noted that in the case of porous PCM, the height of the unit is increased based on the volume of the foam material in order to have similar PCM mass in different cases equal to the PCM only alternative to have a meaningful comparison.

RT54HC has a suitable melting point for domestic usage, especially for the radiator system. The temperatures of radiators are generally in the range of 50-70°C; this is assumed to be at 60°C in this study. RT54HC is also suitable on the account of having a high latent heat of fusion which allows the system to store more thermal energy per unit mass. The properties of RT55HC are presented in Table 1.

Table 1 Physical properties of RT54HC (Rubitherm GmbH)

Property	RT 54HC
Solidus/Liquidus temperature	53/54 (°C)
Latent heat of fusion	200 (kJ/kg)
Specific heat	2.0 (kJ/kg.K)
Solid/Liquid Density	850/800 (kg/m^3)
Thermal conductivity	0.2 (W/m.K)
Viscosity	0.00365 (Pa.s)
Thermal expansion coefficient	0.000308 (1/K)

3. Mathematical description

Without the porous medium, in the PCM solid state, heat is transferred by conduction and then after generating liquid phase, heat is transferred by both conduction and natural convection. In the presence of a porous medium, heat transfer is enlarged by the metal foam inside the PCM rather than low conductivity PCM and the effect of natural convection is negligible (Py et al., 2001). The detailed mathematical modelling and the governing assumptions can be found in (Sardari et al., 2019). A thermal equilibrium model is used to model the effect of porous structure inside the PCM with the aid of an enthalpy-porosity method for the phase change effect. In the thermal equilibrium model, an equal temperature is considered for both the PCM and porous structure. A brief description of the governing equations considering incompressible Newtonian fluid for the PCM in laminar flow regime are as (Sardari et al., 2019):

$$\frac{\partial \rho}{\partial t} + \nabla . \rho \vec{V} = 0 \tag{1}$$

$$\rho \frac{\partial \vec{V}}{\partial t} + \rho(\vec{V}.\nabla)\vec{V} = -\nabla P + \mu(\nabla^2 \vec{V}) - \rho_{ref}\beta\varepsilon(T - T_{ref})\vec{g} - \vec{S} - \vec{F} \tag{2}$$

$$\frac{\partial \varepsilon \rho C_p T}{\partial t} + \nabla(\rho C_p \vec{V} T) = \nabla(k_e \nabla T) - S_L \tag{3}$$

where k_e is defined as the volume average between the thermal conductivities of the porous medium and PCM given as (Liu et al., 2013):

$$k_e = (1 - \varepsilon)k_{porous} + \varepsilon k_{PCM} \tag{4}$$

In the momentum equation, the Boussinesq approximation is employed to consider the effect of natural convection due to the small temperature deference in the domain. Note that the volume expansion of PCM is also neglected during the phase change process. The source term in the momentum equation is given as (Mahdi and Nsofor, 2017):

$$\vec{S} = A_m \frac{(1 - \lambda)^2}{\lambda^3 + 0.001} \vec{V} \tag{5}$$

where A_m is 10^5 (Assis et al., 2007; Ye et al., 2011). The porous medium is also considered open-cell, homogeneous and isotropic. For the PCM-only, the porosity is considered 1 in the governing equations. Additionally, λ is defined as (Al-Abidi et al., 2013):

$$\lambda = \frac{\Delta H}{L} = \begin{cases} 0 & if \;\; T < T_{Solidus} \\ 1 & if \;\; T > T_{Liquidus} \\ \dfrac{T - T_{Solidus}}{T_{Liquidus} - T_{Solidus}} & if \;\; T_{Solidus} < T < T_{Liquidus} \end{cases} \tag{6}$$

where ΔH is the latent heat vary between zero for solid and L is for liquid.

The body force in the momentum equation is defined as (Sardari et al., 2019):

$$\vec{F} = \left(\frac{\mu}{K} + \frac{\rho C\left|\vec{V}\right|}{\sqrt{K}}\right)\vec{V} \tag{7}$$

The formulation related to the calculation of K and C can be found in Ref. (Shahsavar et al., 2019). S_L in the energy equation is defined as (Wang et al., 2015):

$$S_L = \frac{\partial \varepsilon \rho \lambda L}{\partial t} + \nabla\left(\rho \vec{V} \lambda L\right) \tag{8}$$

The rate of heat storage and retrieval can be calculated as the ratio of the storage/retrieval capacity to the melting/solidification time given as (Xu et al., 2017):

$$\begin{aligned} \dot{Q} = \frac{Q}{t_m} &= \frac{m\left(\int_{solid} C_p dT + L_f + \int_{liquid} C_p dT\right)}{t_m} = \frac{m(e_e - e_i)}{t_m} \\ &\approx \frac{m(C_p(T_m - T_i) + \; + L + C_p(T_e - T_m))}{t_m} \end{aligned} \tag{9}$$

It should be noted that in the thermal equilibrium model, the temperatures of the PCM and porous medium are assumed to be similar. This assumption is justified for phase change since most of the phase change process happens when the temperature is almost constant.

4. Charging/discharging mechanism

In the charging process, the LHS unit is fixed at the back of the radiator to gain heat from the radiator back surface with a constant wall temperature. The constant temperature of 60°C is used for the front wall and all the other walls are assumed to be insulated.

For the discharging process, the convection boundary condition is imposed for the front wall with an ambient temperature of 21°C. It is also assumed that no water exists in the radiator's surface and the heat is transferred from the composite PCM to the ambient by aluminium layer of radiator's wall. The convection heat transfer coefficient between the system and ambient is calculated at the film temperature considering the wall temperature at the PCM melting point (54°C). In the laminar range, for a vertical wall, the convection heat transfer coefficient is calculated based on the experimental data (Bejan, 2013):

$$\bar{h} = \frac{k\overline{Nu}}{H} = \frac{k}{H}(0.68 + \frac{0.67Ra^{1/4}}{[1 + (0.492/Pr)^{9/16}]^{4/9}} \quad (10)$$

It is noteworthy that for thermal comfort purposes, according to ASHRAE standard, the ambient air temperature inside the room should be in the range of 19.5°C and 27.8°C which is assumed to be 21°C in this study (Bejan, 2013). The aim is to maintain the room temperature in the range of thermal comfort temperature without turning on the boiler. Therefore, in the charging process, the aim is to find the time that the compact LHS unit is fully charged and the temperature rise on the radiator's surface temperature when the boiler is working. In the discharging mode, the aim is to find if this system can provide a constant temperature for the radiator's surface, and then find the time that the system can provide a constant temperature on the radiator's surface.

5. Numerical modelling and Validation

ANSYS-FLUENT software is utilized to discretise the governing equations using SIMPLE algorithm with double-precision accuracy. PRESTO scheme for pressure correction equation and QUICK scheme for the momentum and energy equations are employed. The values for

under-relaxation factors are set to 0.3, 0.6, 1 and 0.9 for the pressure, velocity, energy and liquid fraction, respectively. The convergence criteria for all the equations are set to 10^{-6}. Fig. 2 displays the entire computational mesh, showing meshes on the front and sides. It includes 100000 (100×100×10) cells with the dense mesh near the walls especially in the y-direction to capture the effect of gravity. Note that due to geometric symmetry, only half of the domain is modelled.

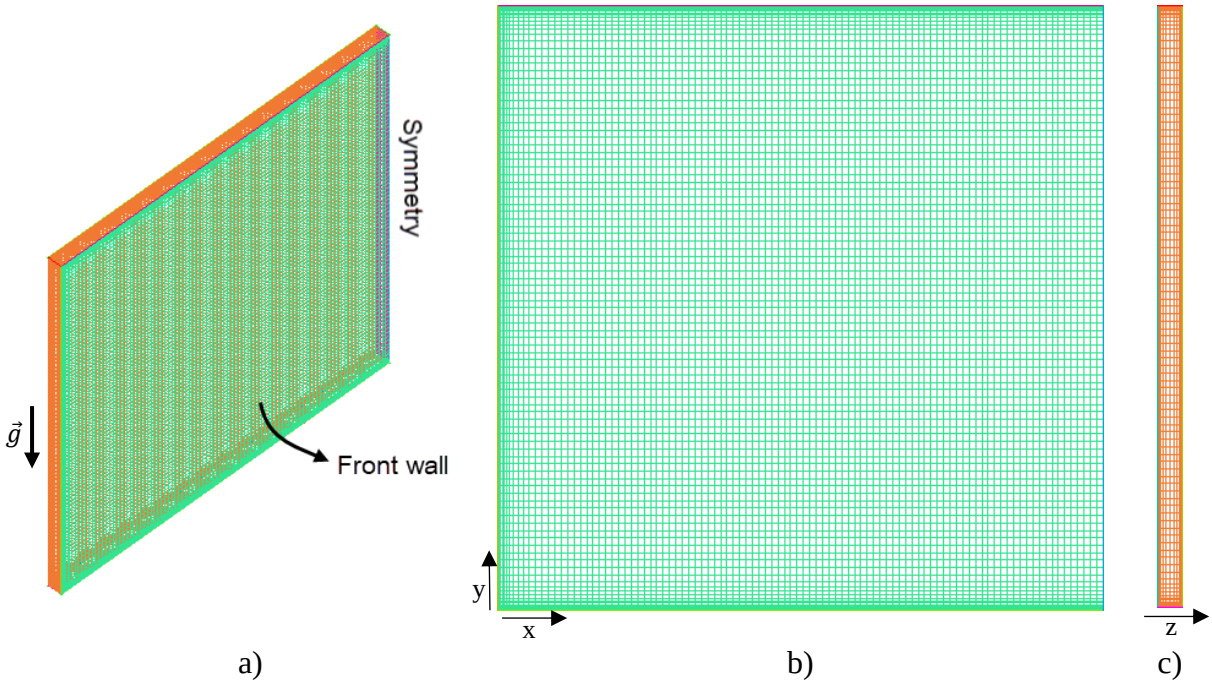

Fig. 2. The schematic of the computation domain with 100000

Different cell sizes are also studied for the grid independency analysis which is presented in Table 2 for the PCM-only alternative. The results show a negligible difference between the results of 144000 elements and 100000 elements cells. Therefore, the grid size of 100000 elements is selected.

Table 2 Effect of elements number on the melting and solidification times

Number of elements	Melting time (h)	Solidification time (h)
64000	19283	74239
100000	20625	76010
144000	20842	76284

Two time-steps of 0.5 and 0.25 s for the grid size of 100000 cells were studied for the porous-PCM case. No significant variation was seen in the variation of charging/discharging. For the PCM-only system, 0.25s is selected for the time step size.

For the porous-PCM simulation, the results of Liu et al. (Liu et al., 2013) are employed to verified the applied model employing a 95% porosity copper foam/PCM using RT-58 in a rectangular enclosure. Fig. 3 illustrates the temperature variation at the height of 8 mm showing an excellent agreement.

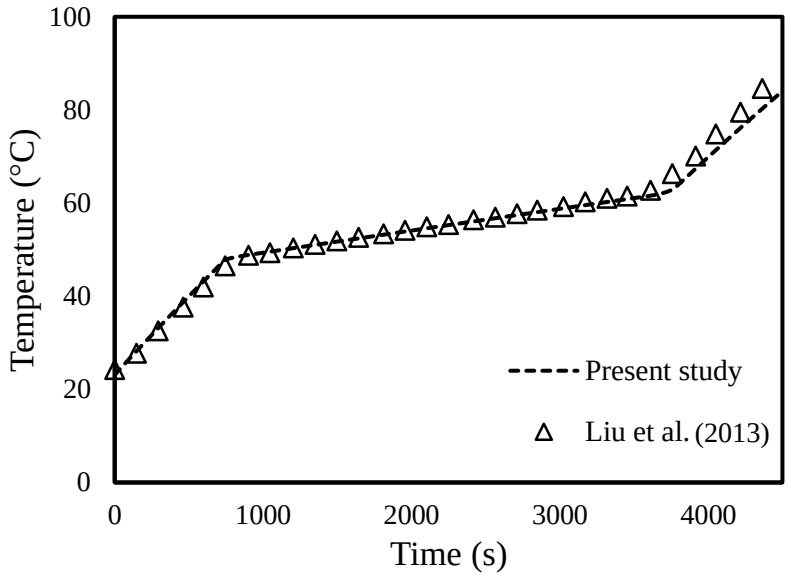

Fig. 3. Code verification compared with the study of Liu et al. (2013)

To study the code validation for the PCM-only alternative, the experimental and numerical results of Mat et al. (Al-Abidi et al., 2013) are employed. Fig. 4 illustrates the average temperature and the liquid fraction a triple tube fined LHS unit showing an excellent agreement.

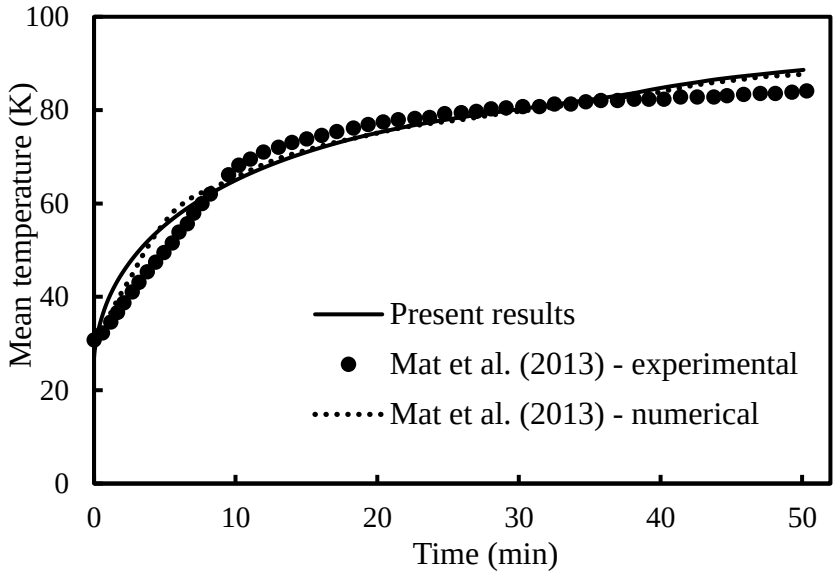

a)

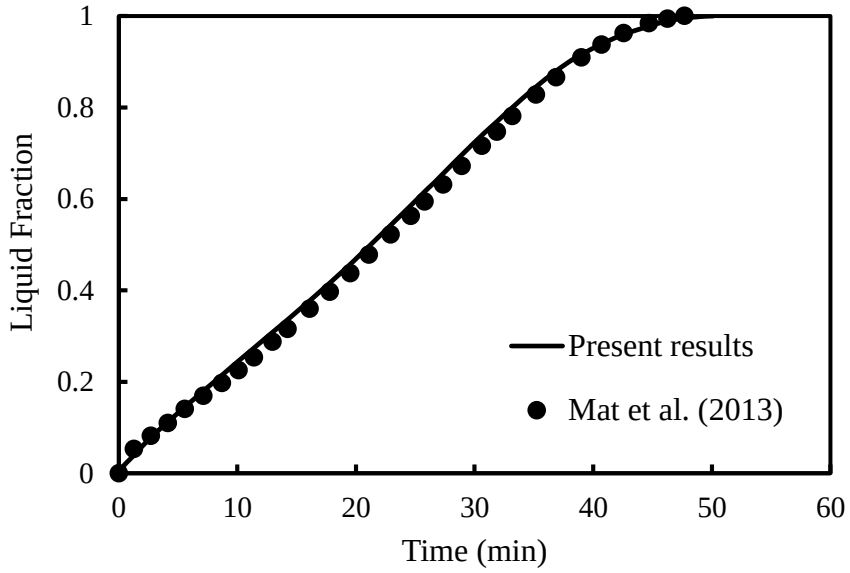

b)

Fig. 4. Code validation for (a) average temperature and (b) liquid fraction of for the PCM-only alternative compared with the study of Mat et al. (2013).

6. Results and discussion

This section is devoted to discussion on the two modes of the unit (the charging and discharging modes) which are discussed as follows:

6.1. Charging mode

In the charging mode, the front wall of the compact LHS unit gains heat from the constant wall temperature of the radiator. During the charging mode, the charging time is a key parameter and a shorter charging time is desirable. After the storing of the heat is complete, the boiler can be turned off and retrieve the heat from the unit to maintain constant room temperature. In this study, three different porosities (95%, 97% and 99%) of the metal foam were examined and compared with the PCM-only alternative.

Fig. 5 display the variation of PCM's average temperature in terms of time for the porous PCM alternatives compared with the PCM-only alternative. The temperature rises rapidly in the porous PCM alternative due to the high conductivity of the metal foam. In the presence of metal foam, the heat is transferred by conduction through the highly conductive porous foam rather than PCM on its own, which enhances the effective thermal conductivity and the rate of thermal diffusion. In the PCM-only alternative, in the beginning, the heat is transferred by conduction through low conductivity PCM. Note that the conductivity of Aluminium and PCM are about 200 and 0.2 W/m.K and the volume average conductivity of the porous PCM is 20.18 W/m.K. In the PCM-only alternative, after the melting part of PCM, natural convection generated in the liquid PCM helps to diffuse heat in the domain. However, as shown, the effect of natural convection in PCM-only alternative is negligible compared with the porous PCM alternative. Note that in the porous PCM alternative, the effect of natural convection is negligible since the porous structure causes the movement of liquid PCM to slow down and thus suppresses the effect of natural convection. For example, if the porosity is 95%, after almost 600s, the PCM temperature rises to the temperature of the front wall (60 ℃) while the same process takes 4h for the PCM-only alternative.

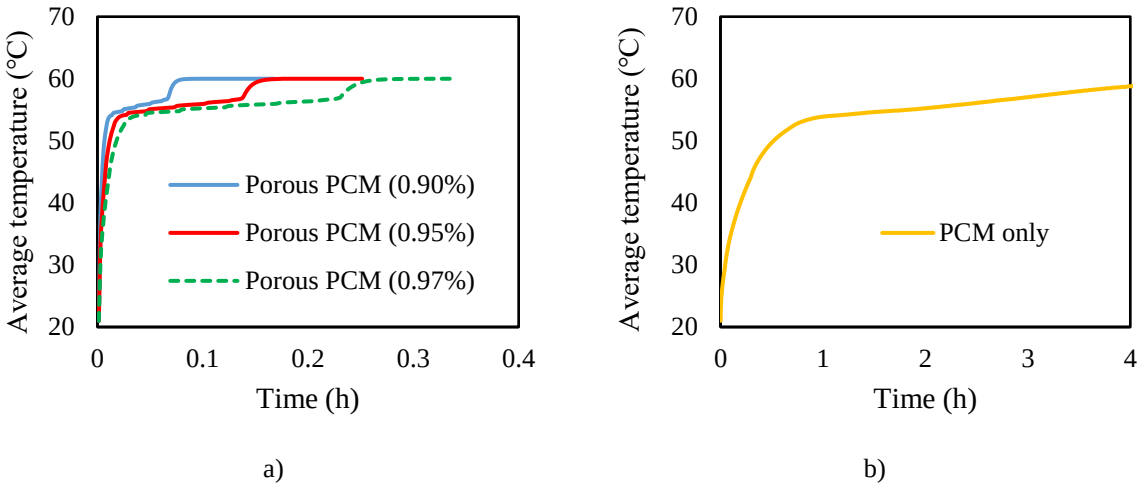

Fig. 5. The variation of PCM average temperature for the cases of a) porous PCM and b) PCM-only

To better understand the effect of metal foam, the variation of temperature at different locations in the x-direction (perpendicular to the front wall) is shown in Fig. 6. Note that x=0cm means the temperature of the front wall, which is constant at 60 ℃. In the porous PCM alternative, due to the presence of high conductivity aluminium foam, the heat transfers very fast. As shown, after 600s, all points have the same temperature similar to the front wall. The temperature rises sharply from the initial temperature (21 ℃) and then remains almost constant during the phase change from solidus temperature (53 ℃) to liquidus temperature (54 ℃), and then again rises sharply. In contrast, in the PCM-only alternative, due to the low thermal conductivity of PCM and low rate of thermal diffusion, the temperature of all points reached 60 ℃ after almost 3.5 h. Furthermore, after almost 1h, the temperatures of different points rise to the solidus temperature, results in starting the phase change process.

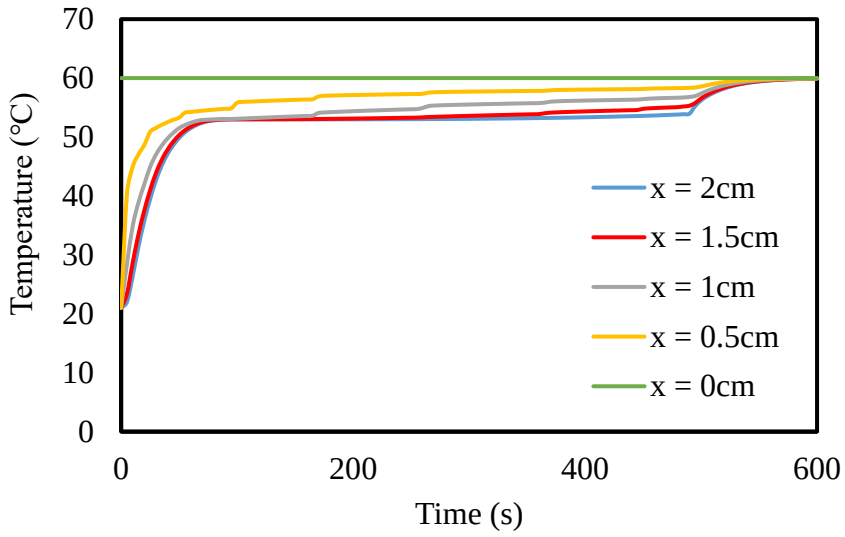

a)

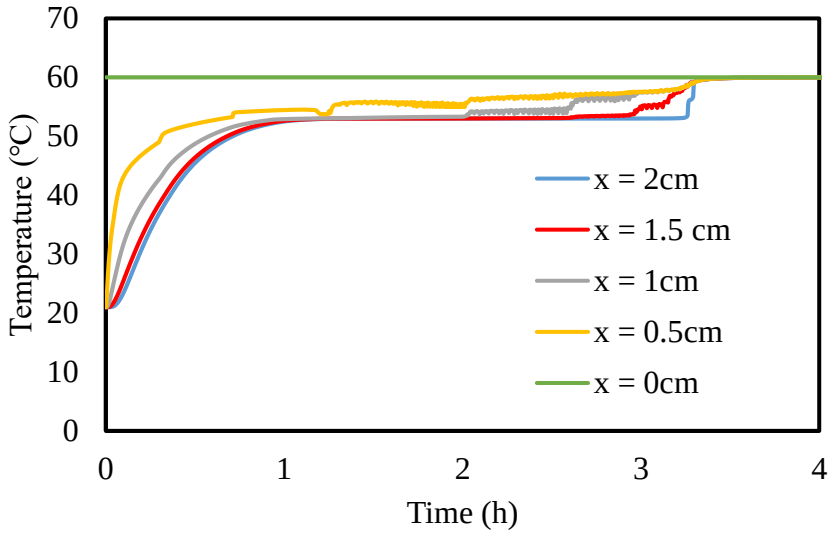

b)

Fig. 6. The variation of PCM temperature at different points in the x-direction for the cases of a) porous PCM (ε=95%) and b) PCM-only

Fig. 7-a: displays the liquid fraction contour plots at the mid-plane section for the porous PCM alternative with the porosity of 95% during charging mode at 100 s intervals and Fig. 7-b illustrates the same plots for the PCM-only alternative at 1h intervals. Note that for the displayed figures, due to the small thickness of the system (2cm), ratios between the width and

height is exaggerated to better show the contour of liquid fraction. The dimensions of the unit as well as the hot surface are shown in the first picture of Fig. 7-a.

Due to the presence of metal foam, as shown in Fig 7-a, the heat is transferred by conduction throughout the system. The interface line between the solid and liquid phase moves from the hot surface (front wall) to the back of the heat storage unit. Note that the interface line is almost smooth due to conduction heat transfer. However, as shown for the PCM-only alternative (Fig. 7-b), natural convection is taking place in the liquid zone helping to transfer heat better in the domain results a non-uniform temperature profile. The liquid PCM moves upward near the hot surface and then generates an anticlockwise circulation by moving downward near the cold solid region. Furthermore, the PCM melts after almost 6h for the PCM-only alternative while after 10 minutes the PCM melts entirely for the porous PCM alternative. Note that for the displayed figure, due to the small thickness of the system (2cm), ratios between the width and height is exaggerated to better show the contour of liquid fraction.

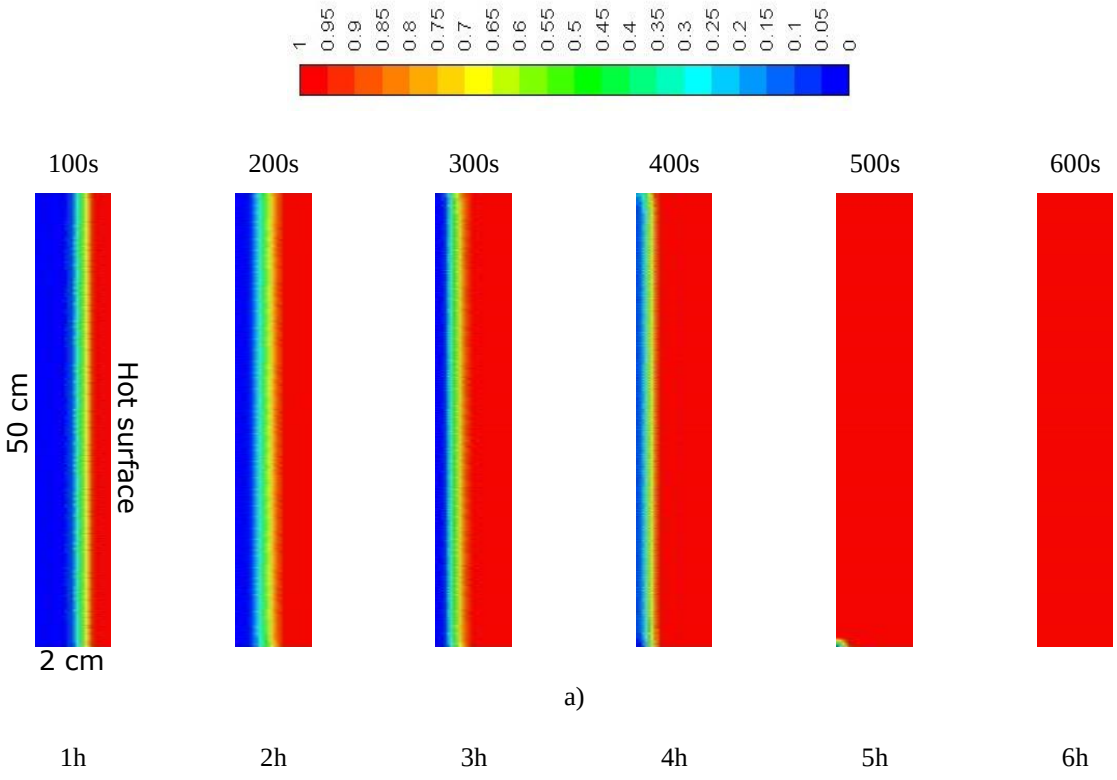

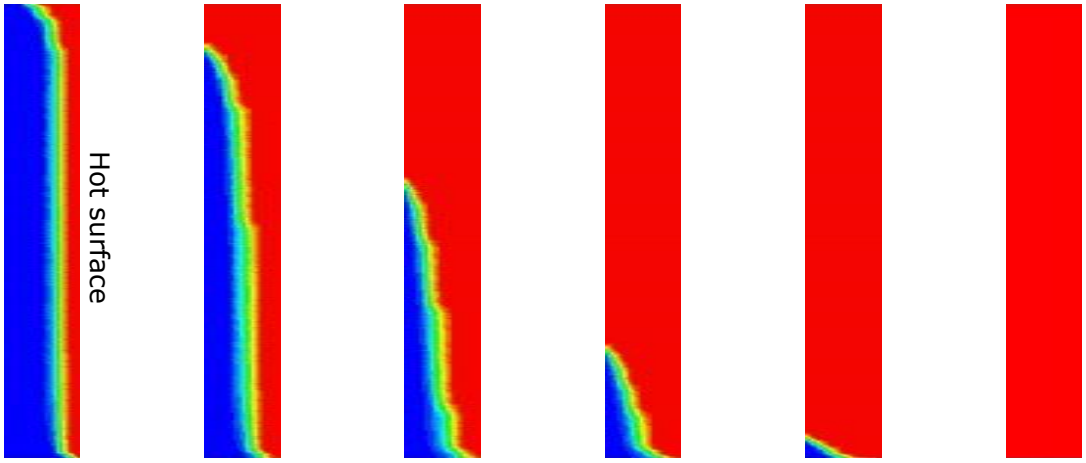

b)

Fig. 7. The contour plot of the liquid fraction for the cases of a) porous PCM and b) PCM-only

Fig. 8 plots the liquid fraction in terms of time for different porous PCM alternatives compared with the PCM-only alternative. The porous PCM alternatives can store heat much faster compared with the PCM-only alternative due to the presence of highly conductive metal foam. Furthermore, due to the small thickness of the compact unit and big surface of the heat source in this application, the heat is transferred rapidly resulting in short charging time.

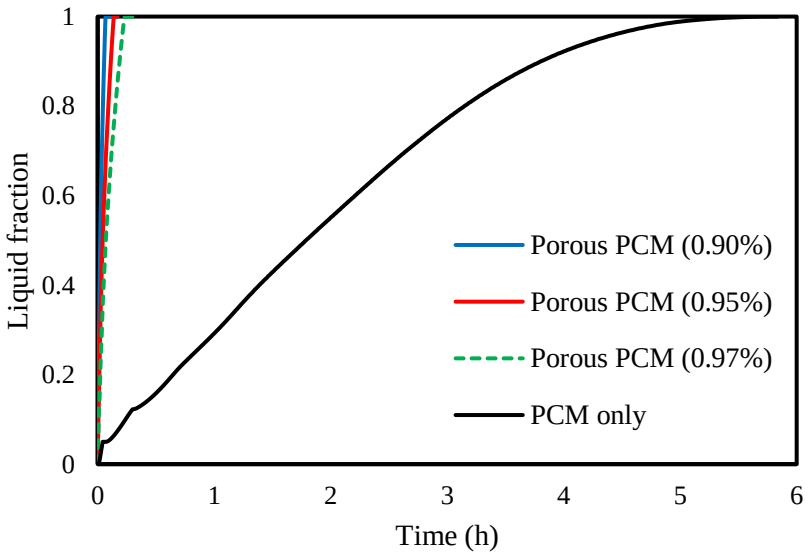

Fig. 8. The variation of the liquid fraction in terms of time for the porous PCM cases with different porosity compared with PCM-only alternative

Table 3 summarizes the charging time, the total heat capacity and the rate of heat storage of the porous PCM alternatives compared with the PCM-only alternative. The percentage of time-saving compared to the PCM-only unit is also presented. According to the Eq. (9), the storage capacity is 2293.5 kJ considering the end point temperature of 60℃ equal to the radiator surface temperature and the initial temperature of 21℃ equal to the comfort temperature of the room. The amounts of heat storage presented in Table 3 for different cases are calculated based on the results of total energy difference in the domain obtained from FLUENT software. The small difference is due to the temperature of the PCM at the end of the simulation, which is slightly different for different cases. Reducing the porosity results in a higher amount of aluminium in the domain which increases the rate of heat transfer and therefore higher heat storage rate is achieved. The rate of heat storage for the porosity of 90% is more than twice of heat storage for the porosity of 95%.

Table 3 The charging time, heat storage capacity and rate of heat storage for different cases

	Charging time (s)	Time-saving compared with PCM-only alternative (%)	Heat storage capacity (kJ)	Heat storage rate (W)
Porous PCM ($\varepsilon = 0.9$)	245	98.8	2262.6	9235.0
Porous PCM ($\varepsilon = 0.95$)	510	97.5	2266.1	4443.3
Porous PCM ($\varepsilon = 0.97$)	875	95.8	2276.7	2601.9
PCM-only	20625	-	2292.8	111.2

Based on the results achieved from this section, it can be concluded that with the help of high conductivity porous medium, almost 2266 kJ thermal energy can be stored in less than 9 minutes. In other words, the CLHS unit uses the thermal energy of the radiator for just 9 minutes which is then used during the discharging process.

6.2. Discharging mode

During the discharging mode, the heat is released to the environment from the front wall. Instead of the constant temperature boundary condition for the front wall during the charging mode, the convection boundary condition was imposed on the front wall in the discharging mode when the room temperature is 21℃. As mentioned, it is assumed that no water exists in the radiator's surface and therefore the boundary is assumed to be aluminium.

Fig. 9 illustrates the variation of PCM's average temperature in terms of time for different cases in the discharging mode. The first sharp drop in the temperature profile is related to the temperature reduction from the initial temperature (60℃) to the liquidus temperature (54℃) when the phase change process has started. For the porous PCM alternatives, during the phase change process, the average temperature is almost constant, namely changing from 54℃ to 53℃. In addition to the influence of the presence of high conductivity porous medium, a small difference between the solidus and liquidus temperature of the PCM material helps to have an almost constant temperature during the phase change process. After that, the temperature drops sharply for the second time. For the PCM-only alternative, the average temperature drops slowly due to the low thermal conductivity of PCM. After 9 hours, the rate of temperature reduction accelerates.

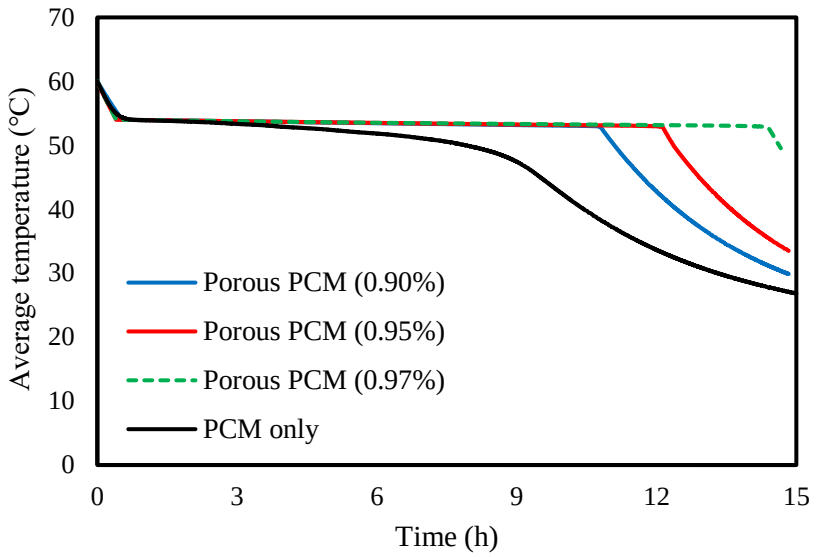

Fig. 9. The variation of PCM average temperature in terms of time for different cases in the discharging process.

Figs. 10-a, 10-b, and 10-c show the variation of temperature at different points in x, y and z directions, respectively, for the porous PCM alternative compared with the PCM-only. The temperatures do not vary significantly at different points for the porous PCM alternative due to the presence of the porous medium. The high conductivity porous medium makes a uniform temperature distribution in the domain. For the PCM-only alternative, except the points in the z-direction, the temperature changes in the x and y-directions. For the points closer to the front wall in the x-direction, a lower temperature is achieved through the time since more heat is released from the PCM. Note that x-direction is perpendicular to the front wall and y-direction is along the gravity direction. In the y-direction, due to buoyancy force and circulation of the liquid PCM, the PCM solidifies from the bottom and therefore the temperature of the point rises from bottom to the top layers of the unit. In both cases, when the liquid fraction reaches to zero at a point, the temperature drops sharply since that point is now placed in the sensible heat part of the discharging mode.

Porous PCM

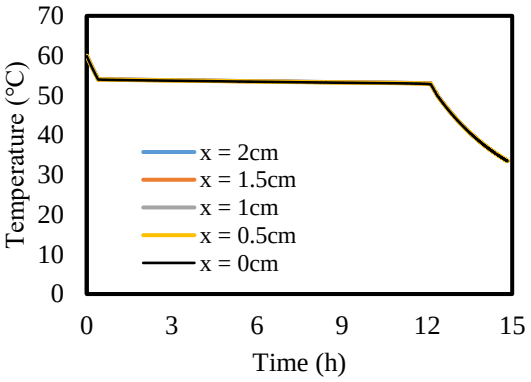

PCM only

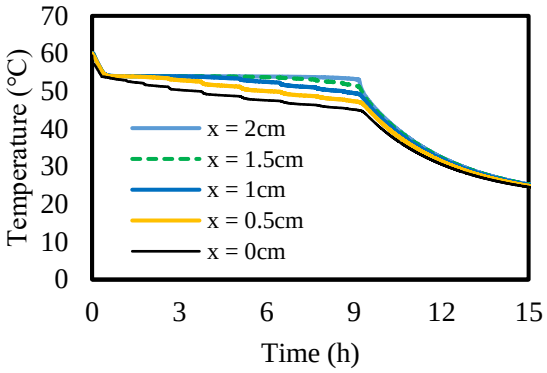

a)

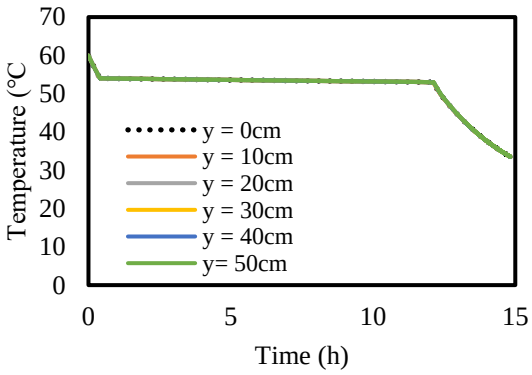

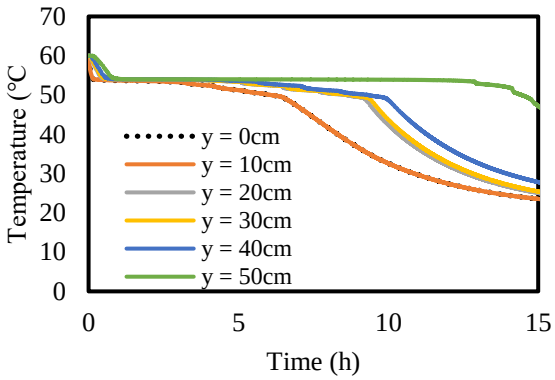

b)

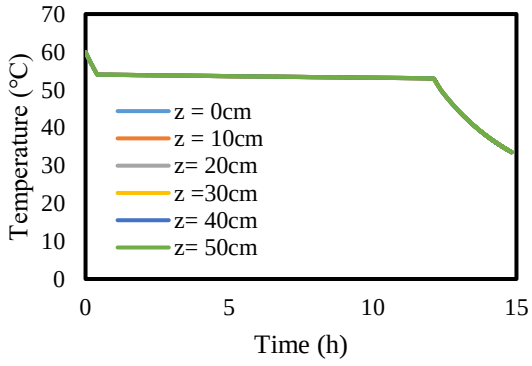

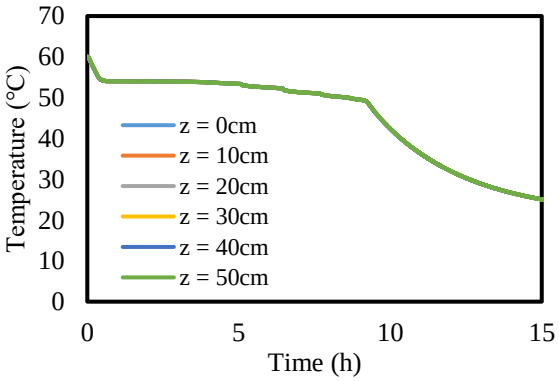

c)

Fig. 10. The variation of temperature at different points in a) x-direction, b) y-direction and c) z-direction for both porous PCM and PCM only systems

Fig. 11 shows the contour plot of the liquid fraction at one-hour time intervals for the porous PCM alternative with the porosity of 95% compared with the PCM-only alternative. Due to the presence of metal foam, a more uniform liquid fraction distribution can be seen for the porous PCM alternative compared with the PCM-only alternative. The heat releases from the front wall to the room which is the right wall in the pictures below. Therefore, PCM starts to solidify from the right region to the left. Due to the presence of porous structure in the porous PCM alternative, the solidification process takes place in all the domain with a lower liquid fraction in the right region due to the employed boundary condition. For the PCM-only alternative, natural convection causes liquid PCM circulation in the domain, which helps the heat transfer.

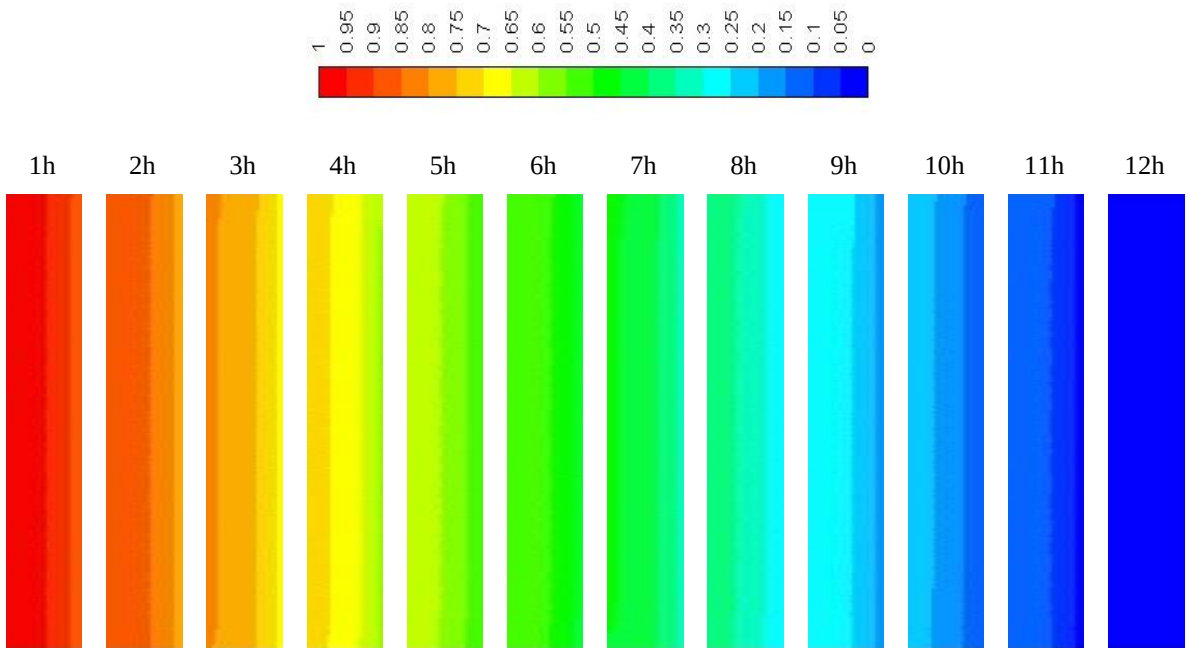

a)

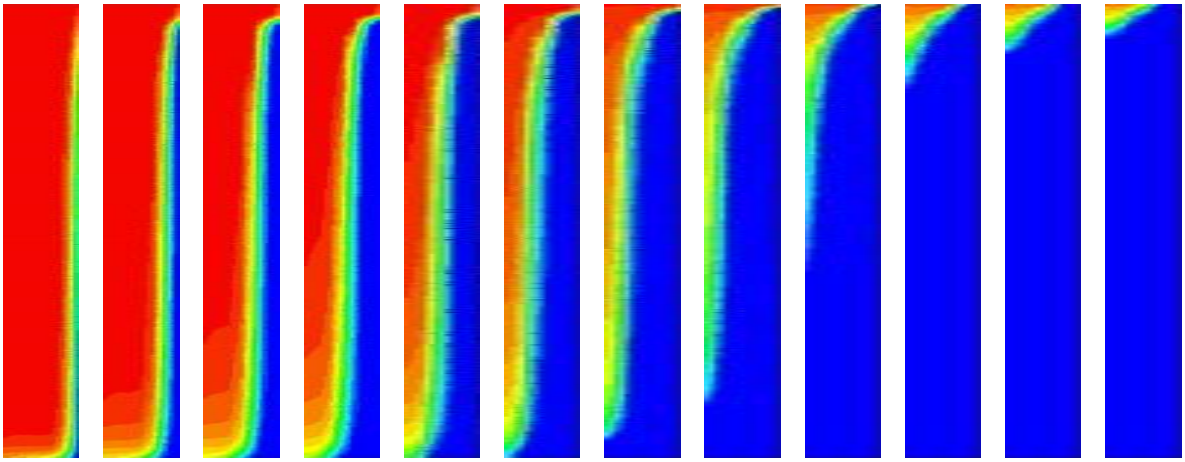

b)

Fig. 11. The contour plots of liquid fraction at one-hour time interval for the cases of a) porous-PCM and b) PCM-only

Fig. 12 plots the liquid fraction for different cases. In contrast to the charging mode when the liquid fraction increases very fast for the porous PCM alternatives, the liquid fraction reduces slowly in the discharging mode. This is because heat is recovered by convection heat transfer mechanism from the compact LHS unit, which is small compared to the case in the charging mode where the relatively high wall temperature is constantly causing a large amount of heat transfer to the domain. Furthermore, the liquid fraction of the porous PCM alternative is higher than that for the PCM-only alternative for the first 10 hours and the total discharging time of the porous PCM alternative is less than PCM-only alternative. Moreover, by reducing the porosity of the metal foam, the discharging time reduces due to a higher amount of heat transfer.

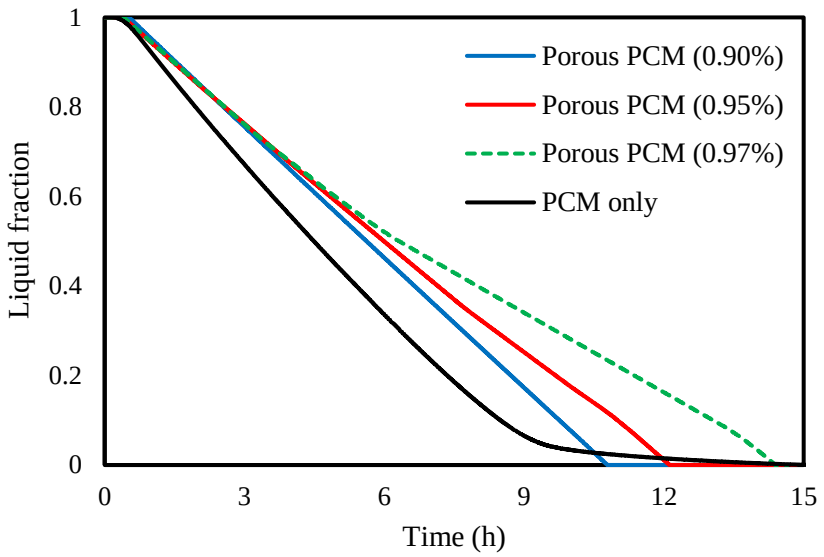

Fig. 12. The variation of liquid fraction in terms of time for different cases

Fig.13 plots the heat flux emitted from the front wall in the symmetry condition in terms of time for different alternatives. The heat flux is almost constant during the phase change process for the porous PCM alternative, which is higher than that for the PCM-only alternative. Furthermore, by increasing the amount of Aluminium in the matrix, higher heat flux exits from the unit. Note that the difference between the emitted heat flux from the porous PCM alternative and PCM-only unit increases through the time.

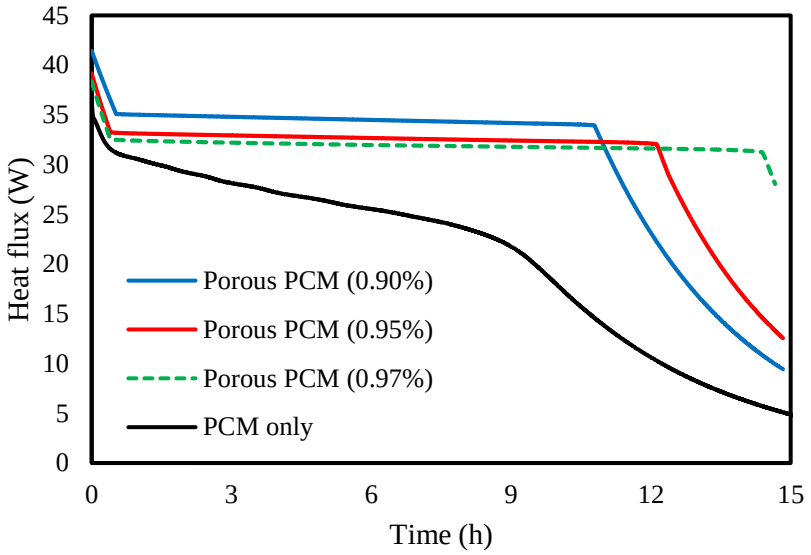

Fig. 13. The variation of emitted heat flux from the front wall for different studied cases in the symmetry condition

Fig. 14 illustrates the average temperature of the front wall of the unit in terms of time for different cases. As shown, for the PCM-only alternative, the wall temperature always reduces. However, for the porous PCM alternatives, the unit surface temperature is kept constant until the end of the solidification process. Therefore, the system is capable of providing a constant temperature on the unit surface. As mentioned, the masses of PCM for different cases are kept constant. As shown in Fig. 13, for the lower porosity, a higher amount of heat flux is emitted from the front surface and therefore as shown in Fig. 12, the discharging time of the system with lower porosity is less. However, as shown in Fig.14, all porous PCM units can provide a constant temperature for the front wall during the discharging time. Therefore, a system with a higher porosity is always preferable.

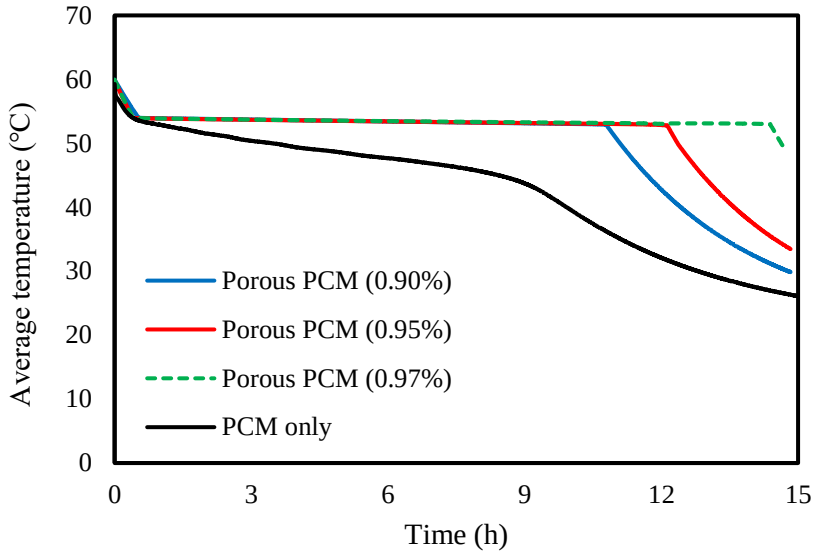

Fig. 14. The average temperature of the front wall in terms of time for different studied cases

Table 4 summarizes the discharging time, the total heat retrieval capacity and rate of heat retrieval from the porous PCM alternative compared with the PCM-only alternative. The percentage of time-saving compared to the PCM-only unit is also presented. Note that the amount of heat recovery capacity is calculated until the liquid fraction reaches zero. For the PCM-only alternative, since the heat transfer process happens slowly from the right side of the storage unit to the left side due to low thermal conductivity of the PCM, the PCM uses the latent and sensible heat simultaneously, has a lower mean PCM temperature at the end of the solidification process occurs and a higher amount of heat retrieval capacity is achieved. However, in the porous-PCM alternative, due to the presence of the porous medium, the PCM solidifies entirely, therefore after the heat recovery process, the temperature is equal to the solidus temperature. The rate of heat retrieval enhances by using a metal foam with lower porosity with a negligible capacity input.

Table 4 The discharging time, heat retrieval capacity and rate of heat retrieval for different cases

	discharging time (h)	Time-saving compared with PCM-only case (%)	Heat retrieval capacity (kJ)	Heat retrieval rate (W)

Porous PCM (ε = 0.9)	10.97	48.01	-2143.4	-44.8
Porous PCM (ε = 0.95)	12.32	41.67	-2145.8	-39.9
Porous PCM (ε = 0.97)	14.79	29.96	-2157.0	-33.4
PCM-only	21.11	0	-2671.8	-29.0

In the discharging mode, it can be concluded that the stored heat in the charging mode is released to the air in almost 12 hours which can provide a uniform temperature on the surface of the radiator similar to the existence of hot water. From Figure 14 porous medium in the energy storage unit provides a uniform temperature on the front wall, whereas without the foam, temperature constantly decreases.

In reality, different types of radiators are employed for space heating. For a typical radiator, water tubes are placed at the external surface and cover almost 50% of the surface, the other 50% consisting of bonded metallic plate separating the vertical water channels. Therefore, for the proposed energy storage unit, for almost 50% of the unit, a layer of water exists between the composite PCM and air. The presence of the water layer, on one hand, reduces the surface temperature of the front wall when a convection boundary condition is considered (for 50% of the unit). On the other hand, it reduces the released heat from the PCM to the air causing a higher solidification time. Therefore, to better understand the effect of the intermittent water layer on the performance of the unit, a 2-D simulation is performed considering the porous PCM (with 95% porosity) with the same dimensions (2 cm × 50cm) with a unit depth and a water layer with 1 cm thickness and the same height. The boundary conditions are considered similar to the 3-D simulation mentioned is section 2. Fig. 15 illustrates the variation of mean temperature for the PCM, water, mid-wall between the PCM and water as well as front wall. The solidification time increases to 36.26 h due to the presence of the water layer. The maximum difference between the temperature of the water-separated front wall (facing room air) and mid-wall (facing PCM and foam) is less than 2ºC. Due to the presence of high

conductivity porous medium and also small thickness of the PCM container, the average temperature of the PCM and mid-wall is almost the same.

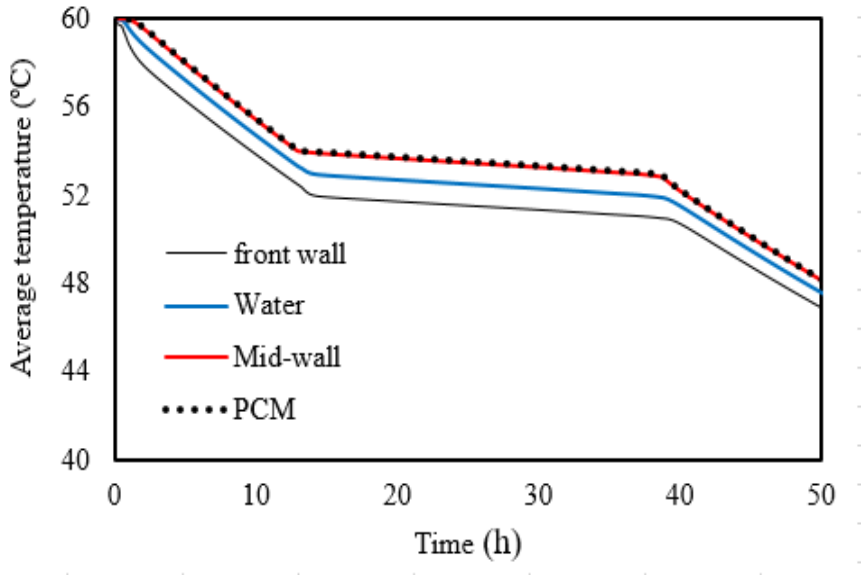

Fig. 15. The effect of considering a water tube between the CLHS unit and the air on the mean temperatures of PCM, water, mid-wall and front wall

~~As a summary, this paper shows the capability of the CLHS system with the aid of porous medium on recovering energy from the typical radiators and then releasing the stored heat to the room helping the peak shaving and energy saving.~~ The energy stored in the unit comes from the radiator which affects the performance of the radiator and also the room, the energy otherwise lost to the walls is captured and insulated in order to have slow release of this back to the radiator at a later time. ~~This study introduces the potential of a novel product especially for peak shaving and also the ability to gain the excess energy of a radiator since more heat loss is occurred from the back surface of the radiator through the room cavity which can be stored in the product. The experimental study should be performed to better understand the behaviour of the unit in a room as the future studies. Also, the amount of more energy that the~~

~~radiator consumes as well as the reduced heat loss from the room when energy storage is placed should be considered for the final design.~~

7. Conclusion

~~As a summary, this paper shows the capability of the CLHS system with the aid of porous medium on recovering energy from the typical radiators and then releasing the stored heat to the room helping the peak-shaving and energy saving.~~~~A compact latent heat storage (CLHS) unit mounted on current commercially available radiators was designed and simulated for space heating.~~ The idea of using the CLHS unit in the back of the radiator is introduced ~~for the first time~~ to demonstrate ~~such~~ that the combination can provide a uniform temperature on the radiator's surface when the boiler is turned off. A high conductivity porous medium ~~is used to~~ enhances the heat transfer inside the PCM. The existence of a porous medium, as well as the 'almost constant' melting temperature of the PCM, helps to provide a uniform temperature in the discharging mode. Different porosities of the metal foam were examined compared to the PCM-only alternative in order to compare material usage and size of heat store. ~~It is concluded that t~~The CLHS unit ~~can~~ provides a constant temperature on the unit surface for almost 11 hours. The charging time for the porous PCM alternatives simulated is less than 15 mins due to the big surface area of the heat source and the presence of metal foam. For the PCM-only alternative, the charging and discharging times are almost 5.7 h and 21 h, respectively. During the discharging process, the surface temperature reduces continuously for the PCM-only alternative. The results of this study lay the foundation for a novel design of a compact unit for energy consumption reduction for space heating used in buildings. The ~~novel~~ product idea developed in this study helps energy-saving and peak-shaving in buildings ~~which results in a cleaner society toward~~with consequents improvement for~~ing~~ environmental sustainability. ~~For~~

~~the future work, the authors will perform the e~~Experimental investigations to practically support the results of this study are now required as a step toward commercializing the product.

References

Al-Abidi, A.A., Mat, S., Sopian, K., Sulaiman, M.Y., Mohammad, A.T., 2013. Internal and external fin heat transfer enhancement technique for latent heat thermal energy storage in triplex tube heat exchangers. Applied Thermal Engineering 53(1), 147-156.

Assis, E., Katsman, L., Ziskind, G., Letan, R., 2007. Numerical and experimental study of melting in a spherical shell. International Journal of Heat and Mass Transfer 50(9), 1790-1804.

BEIS, March 2017. 2016 UK GREENHOUSE GAS EMISSIONS, PROVISIONAL FIGURES. Department for Business, Energy & Industrial Strategy (BEIS).

Bejan, A., 2013. Convection heat transfer. John wiley & sons.

BIES, July 2017. Energy Consumption in the UK. Department of Business, Energy, and Industrial Strategy (BIES).

Campos-Celador, Á., Diarce, G., Zubiaga, J.T., Bandos, T.V., García-Romero, A.M., López, L., Sala, J.M., 2014. Design of a finned plate latent heat thermal energy storage system for domestic applications. Energy Procedia 48, 300-308.

Dadollahi, M., Mehrpooya, M., 2017. Modeling and investigation of high temperature phase change materials (PCM) in different storage tank configurations. Journal of Cleaner Production 161, 831-839.

Dechesne, B., Gendebien, S., Martens, J., Lemort, V., 2014. Designing And Testing An Air-PCM Heat Exchanger For Building Ventilation Application Coupled To Energy Storage, 15th International Refrigeration and Air Conditioning Conference. Purdue,.

Irshad, K., Habib, K., Saidur, R., Kareem, M.W., Saha, B.B., 2019. Study of thermoelectric and photovoltaic facade system for energy efficient building development: A review. Journal of Cleaner Production 209, 1376-1395.

Jamekhorshid, A., Sadrameli, S.M., Farid, M., 2014. A review of microencapsulation methods of phase change materials (PCMs) as a thermal energy storage (TES) medium. Renewable and Sustainable Energy Reviews 31, 531-542.

Khan, Z., Khan, Z., Ghafoor, A., 2016. A review of performance enhancement of PCM based latent heat storage system within the context of materials, thermal stability and compatibility. Energy Conversion and Management 115, 132-158.

Liu, Z., Yao, Y., Wu, H., 2013. Numerical modeling for solid–liquid phase change phenomena in porous media: Shell-and-tube type latent heat thermal energy storage. Applied Energy 112, 1222-1232.

Mahdi, J.M., Nsofor, E.C., 2017. Melting enhancement in triplex-tube latent heat energy storage system using nanoparticles-metal foam combination. Applied Energy 191, 22-34.

Mahdi, J.M., Nsofor, E.C., 2018. Multiple-segment metal foam application in the shell-and-tube PCM thermal energy storage system. Journal of Energy Storage 20, 529-541.

Marique, A.-F., De Meester, T., De Herde, A., Reiter, S., 2014. An online interactive tool to assess energy consumption in residential buildings and for daily mobility. Energy and Buildings 78, 50-58.

Mesalhy, O., Lafdi, K., Elgafy, A., Bowman, K., 2005. Numerical study for enhancing the thermal conductivity of phase change material (PCM) storage using high thermal conductivity porous matrix. Energy Conversion and Management 46(6), 847-867.

Nithyanandam, K., Pitchumani, R., 2014. Computational Studies on Metal Foam and Heat Pipe Enhanced Latent Thermal Energy Storage. Journal of Heat Transfer 136(5), 051503-051503-051510.

Osterman, E., Butala, V., Stritih, U., 2015. PCM thermal storage system for ‘free’ heating and cooling of buildings. Energy and Buildings 106, 125-133.

Pereira da Cunha, J., Eames, P., 2016. Thermal energy storage for low and medium temperature applications using phase change materials – A review. Applied Energy 177, 227-238.

Py, X., Olives, R., Mauran, S., 2001. Paraffin/porous-graphite-matrix composite as a high and constant power thermal storage material. International Journal of Heat and Mass Transfer 44(14), 2727-2737.

Rubitherm GmbH, RT54HC data sheet.

Sarbu, I., Sebarchievici, C., 2016. Solar Heating and Cooling Systems: Fundamentals, Experiments and Applications. Elsevier Science.

Sardari, P.T., Walker, G.S., Gillott, M., Grant, D., Giddings, D., 2019. Numerical modelling of phase change material melting process embedded in porous media: Effect of heat storage size. PROCEEDINGS OF THE INSTITUTION OF MECHANICAL ENGINEERS PART A-JOURNAL OF POWER AND ENERGY.

Shahsavar, A., Al-Rashed, A.A.A.A., Entezari, S., Sardari, P.T., 2019. Melting and solidification characteristics of a double-pipe latent heat storage system with sinusoidal wavy channels embedded in a porous medium. Energy 171, 751-769.

Shang, B., Hu, J., Hu, R., Cheng, J., Luo, X., 2018. Modularized thermal storage unit of metal foam/paraffin composite. International Journal of Heat and Mass Transfer 125, 596-603.

Sheikholeslami, M., 2018a. Numerical modeling of nano enhanced PCM solidification in an enclosure with metallic fin. Journal of Molecular Liquids 259, 424-438.

Sheikholeslami, M., 2018b. Numerical simulation for solidification in a LHTESS by means of Nano-enhanced PCM. Journal of the Taiwan Institute of Chemical Engineers 86, 25-41.

Sheikholeslami, M., Mahian, O., 2019. Enhancement of PCM solidification using inorganic nanoparticles and an external magnetic field with application in energy storage systems. Journal of Cleaner Production 215, 963-977.

Wang, P., Wang, X., Huang, Y., Li, C., Peng, Z., Ding, Y., 2015. Thermal energy charging behaviour of a heat exchange device with a zigzag plate configuration containing multi-phase-change-materials (m-PCMs). Applied Energy 142, 328-336.

Wang, X., Liu, J., Zhang, Y., Di, H., Jiang, Y., 2006. Experimental research on a kind of novel high temperature phase change storage heater. Energy conversion and management 47(15-16), 2211-2222.

Wang, Y.-H., Yang, Y.-T., 2011. Three-dimensional transient cooling simulations of a portable electronic device using PCM (phase change materials) in multi-fin heat sink. Energy 36(8), 5214-5224.

Xiao, X., Zhang, P., Li, M., 2013. Preparation and thermal characterization of paraffin/metal foam composite phase change material. Applied energy 112, 1357-1366.

Xu, Y., Ren, Q., Zheng, Z.-J., He, Y.-L., 2017. Evaluation and optimization of melting performance for a latent heat thermal energy storage unit partially filled with porous media. Applied energy 193, 84-95.

Ye, W.-B., Zhu, D.-S., Wang, N., 2011. Numerical simulation on phase-change thermal storage/release in a plate-fin unit. Applied Thermal Engineering 31(17), 3871-3884.

Yong, J.Y., Klemeš, J.J., Varbanov, P.S., Huisingh, D., 2016. Cleaner energy for cleaner production: modelling, simulation, optimisation and waste management. Journal of Cleaner Production 111, 1-16.

Yu, Z., Gou, Z., Qian, F., Fu, J., Tao, Y., 2019. Towards an optimized zero energy solar house: A critical analysis of passive and active design strategies used in Solar Decathlon Europe in Madrid. Journal of Cleaner Production 236, 117646.

Zhang, P., Meng, Z.N., Zhu, H., Wang, Y.L., Peng, S.P., 2017. Melting heat transfer characteristics of a composite phase change material fabricated by paraffin and metal foam. Applied Energy 185, 1971-1983.

Zhao, C., 2012. Review on thermal transport in high porosity cellular metal foams with open cells. International Journal of Heat and Mass Transfer 55(13-14), 3618-3632.

Zhao, C.Y., Lu, W., Tian, Y., 2010. Heat transfer enhancement for thermal energy storage using metal foams embedded within phase change materials (PCMs). Solar Energy 84(8), 1402-1412.